COMPUTER-AIDED DESIGN & APPLICATIONS, 2018
VOL. 15, NO. 4, 532–541
https://doi.org/10.1080/16864360.2017.1419641

Linkage-FFD algorithm for dental crown and abutment shape design

Xun Li [a] and Ming Chen [b]

[a]Shenzhen Graduate School, Harbin Institute of Technology, China; [b] School of Computer Science and Information Technology, Guangxi Normal University, China

ABSTRACT
In dental CAD, crown design is one core function and the thickness between the crown and the corresponding abutment should be in the standard range. However, the thickness requirement is currently not considered when designing the crown. In this paper, a novel algorithm, i.e., linkage free-form deformation (L-FFD) is proposed to automatically ensure the thickness requirement in the crown design. The algorithm of the direct manipulation of free-form deformation (DMFFD) [3] is implemented to support the crown design, and three more steps, i.e., local adjustment by DMFFD, thickness detection and smoothing, are performed on the abutment alternately and iteratively, which will make sure the abutment is smooth and at the same time the thickness requirement is automatically met. As the thickness requirement varies at different parts of a tooth, the local coordinate system is established in this paper to help quickly classify the vertices of the tooth. The algorithm is implemented and the tested examples show that it is efficient and valid, which can speed up the crown design by saving the manual modification of abutment for satisfying the thickness requirement.

KEYWORDS
Dental CAD; crown design; free form deformation; abutment design

1. Introduction

Dental CAD system [5], [11] has been widely used in clinical trials, greatly improving the success rate of surgery and shortening the operation cycle. For dental CAD, one of core functions is to model the crown shape, which can be divided into two categories, i.e., inlay/onlay modeling and full crown modeling. In current dental CAD package, designing a crown includes two steps: 1) first take a corresponding standard tooth from the database and 2) repeatedly fine-edit it using shape deformation algorithm to obtain the final ideal shape. Steinbrecher [13] first designed the inlay based on the iterative laplacian algorithm [6], [14]. On this basis, Zhang [17] and Jiang [4] further improved the algorithm and used it to design inlays and full crowns. Due to the tooth's daily wear, blindly retaining all the details of the standard teeth during the deformation may result in morphological gap between the designed crown and its jaw-paired counterpart. In order to solve this problem, Blanz [1] uses the standard tooth as the template to manually select the tooth residual information for inlay/onlay repair; Zheng [18] uses the standard method to take the interactive way and take the radial basis function deformation algorithm to complete the crown design. However, the above two methods are both required to interactively specify feature points for matching; if the feature points are not accurately located, matching distortion occurs and then design fails. As human teeth are anatomically similar from each other, Mehl [9] designed the Biogeneric tooth for the restoration of inlay/onlay from the statistical point of view based on the principal component analysis. Boigeneric tooth is an approximately fitting method and lots of adjustment time is needed for obtain a fine tooth surface.

So far, although lots of research work has been done on the crown design, these studies only focus on the outer surface design of the crown, not synchronically considering the thickness between the designed crown and its abutment (the designed crown will further be glued to the abutment). In the crown design, meeting the standard thickness is a must [7]. As far as we know, all dental CAD systems complete the design of a crown without thickness consideration and the abutment-crown thickness requirement is guaranteed later by mutually adjusting the abutment shape with great care [8] or even repeatedly modifying the shape of the already designed crown. This method requires more operating time and skilled experiences, and sometimes the trade-off between the crown thickness and crown shape should be made. If this compromise is not properly dealt with, cervical margin

CONTACT Xun Li lx_hit@163.com; Ming Chen hustcm@hotmail.com

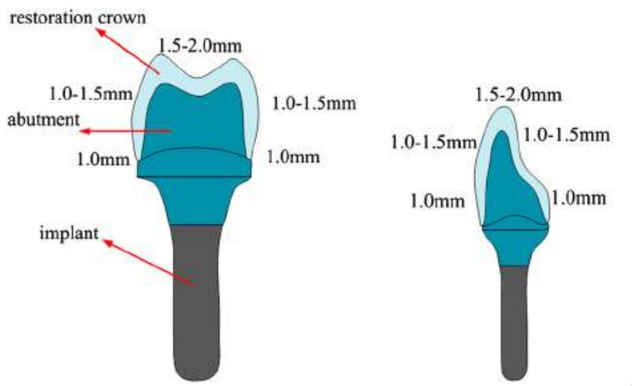

Figure 1. The thickness distribution requirement for different parts of crowns.

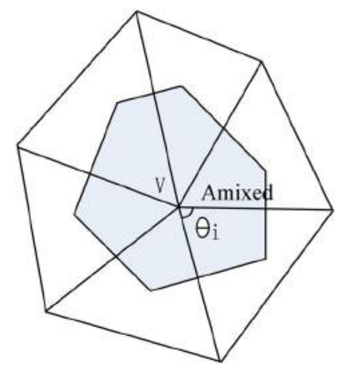

Figure 2. Three parameters when evaluating the discrete Gaussian curvature at vertex *V*.

collapse may occur or the high quality occlusal morphology is difficult to obtain. The thickness between the abutment and corresponding crown should be in the range [2] shown in Fig. 1.

From Fig. 1, we can find that the thickness requirement is varied at different parts of the crown: the thickness of the axial surface part is $1.0 \sim 1.5$, but the thickness of the occlusal surface part is relatively thicker ($1.5 \sim 2.0$ mm) due to bear the bite function. Too less thickness amount will result in tooth's strength not being enough, but too large thickness number may cause the sintering problem. Besides the thickness requirement, the abutment should hold the similar anatomical shape with the designed crown, which is conducive to further porcelain process and good mechanical properties. The designed crown's inside shape is nearly the same with the abutment shape and 0.05 mm gap between them is made for adhesive to glue the crown and abutment together. In other words, once the shape of abutment is determined and the inner shape of the crown can be directly made from the abutment by surface-offset operating.

2. Establishment of local coordinate system

As mentioned before, different part of tooth needs various thickness numbers, so it need to first determine the part classification of all vertices of the crown mesh model. Thus, we first establish a local coordinate system for each single tooth, which will be used in the vertex classification.

Anatomically, each tooth can split into six sides [15]: medial and distal sides, buccal and lingual sides, and gingival and occlusion sides. Although these sides have been anatomically defined, they have not been well presented in geometric terms. Therefore, in establishing a coordinate system, the feature point of each side must be taken into consideration: the bumps found in buccal and lingual sides and the contact points presented on both the medial and distal sides allow for the establishment of a coordinate system.

In general, bumps are more visually obvious than contact points and also easier to be selected and located, so it is natural to rely on the bumps to establish a coordinate system. The method of semi-interactive extraction feature points (SEF) is now proposed. This involves the user firstly assigning a fuzzy region within the system so that the system may automatically extract its associated feature points. This fuzzy region is a circular region featuring a center point that is defined by the current mouse selection point with a radius of 2 mm. As this feature point is represented as a local peak point, it will have the largest absolute value of Gaussian curvature. In consideration of the fine-mesh nature of the scanned model, the discrete Gaussian curvature will be evaluated by (2.1).

$$k_G(v) = 2\pi - \sum_{j=1}^{n} \theta_j / A_{mixed} \tag{2.1}$$

Fig. 2 shows the parameters of formula (2.1): n is the number of triangles in the one-link neighborhood, A_{mixed} is the total Voronoi area shaded in cyan color, and θ_j is the angle of at vertex V of the incident triangle.

Based on SEF, the local coordinate system of the tooth could be established in the steps given below (see Fig. 3):

1) Use the SEF method to derive four feature points marked as A, B, C, and D in the buccal and lingual sides and medial and distal sides, respectively.
2) Connect A and B to achieve line AB and connect C and D to achieve line CD. The gingival to occlusion direction can be determined via the cross product of AB and CD. This direction is marked as the Z axis of the coordinate system.
3) Project line CD into the plane that passes through line AB and takes Z as the normal direction. The

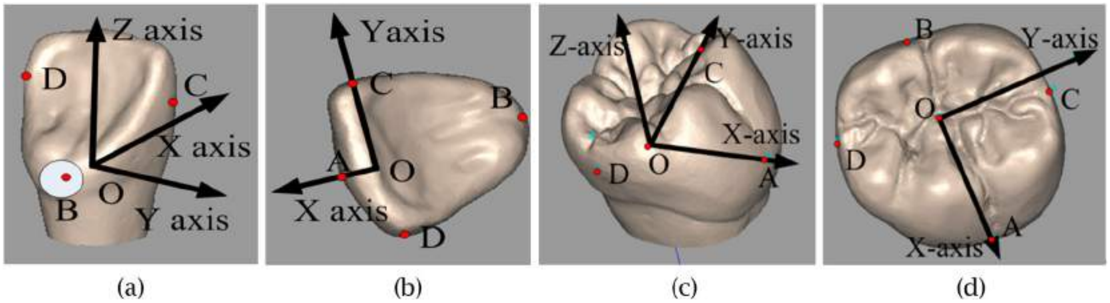

Figure 3. Build the local coordinate system for the input incisor and molar model: (a) the isometric view of incisor;(b)the top view of incisor;(c) the isometric view of molar;(d) the top view of molar.

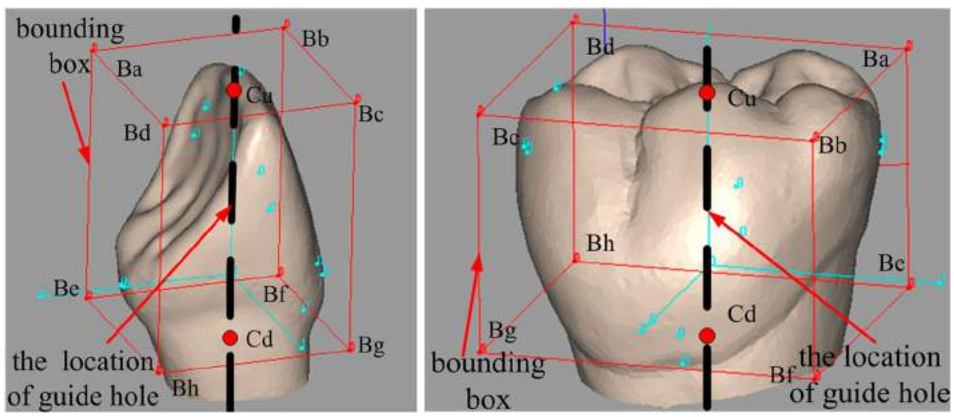

Figure 4. These bounding boxes for (a) an incisor and (b) a molar.

intersection point between the projections of CD and AB is then taken as the origin O of the coordinate system.

4) AB is marked as the X axis. Y axis is derived from the cross product of the X and Z axes.

The aforementioned steps elucidate the establishment of tooth coordinates. Fig. 5 demonstrates the coordinates of an incisor and a molar established via the use of developed dental CAD.

Each coordinate axis represents one certain anatomical plane in the dental CAD system. In this system, the Z axis is perpendicular to the occlusion and gingival plane, the X axis is perpendicular to the buccal and lingual planes and the Y axis is perpendicular to medial and distal planes, respectively. In Fig. 3 (a), the SEF method demonstrates that the white circular region is represented as an area assigned by the user, whereas the red point is a featured point calculated with local maximum Gaussian curvature.

The six planes of the constructed bounding box can approximately represent six anatomical surfaces. The classification of vertices can be simply determined in a simple way: connect each vertex and the origin of the local coordinate as one line segment, which will hit one plane of the bounding box; if the intersection point is on the top plane, this vertex will belong to the occlusal surface part, otherwise it belong to the axial surface. Fig. 4 shows these bounding boxes for two teeth.

3. Acquisition of the initial abutment

For each standard tooth, one abutment is pre-designed and its shape will be automatically deformed according to the modification of the crown. As tooth possesses complicated features such as grooves, ridges and cusp, constructing an abutment from its corresponding standard tooth by surface-offsetting operator usually causes geometric collisions among these features. In this paper, the initial abutment is obtained in a step-by-step manner: first scale down the initial crown and then smooth it to remove detailed features for the easiness of smearing adhesives. More explicitly, the standard tooth model is noted as $M = (C, V)$ where C is the topological connection among vertices, edges and triangles of M and $V = \{v_1, v_2, \cdots, v_n\}$ represents the vertices of M. The mesh model of the initial abutment is denoted as $M' = (C', V')$ and let $C' = C$, which means that M’ has the

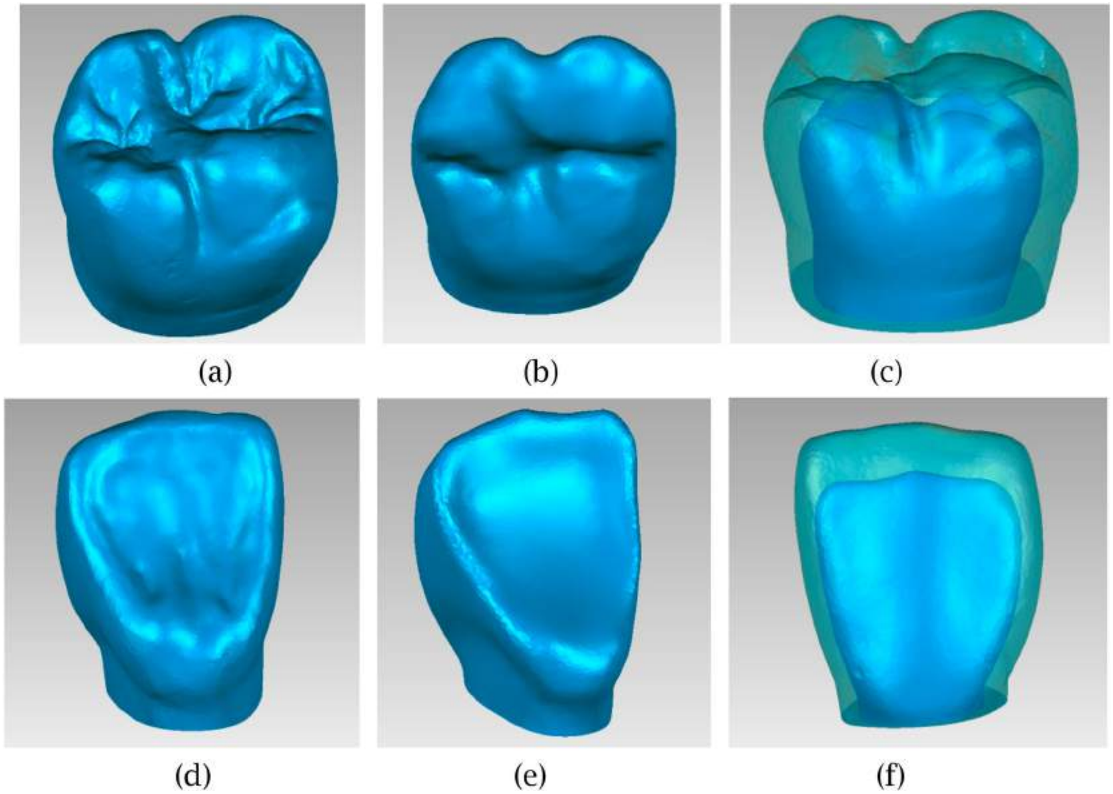

Figure 5. The resultant initial abutment by the proposed algorithm: (a) The standard molar tooth, (b) The obtained initial abutment for the molar, (c) The molar is set on the abutment, (d) The standard incisor tooth, (e) The obtained initial abutment for the incisor, (f) The incisor is set on the abutment.

same number of vertices, edges, triangles and topological connection with those of M. As the reasonable thickness between M and M' should be kept, M' can be achieved via shrinking the x and y coordinate of all vertices of M by $D_{axial} \in (1.2, 1.3)$ and z coordinates by $D_{occlusion} \in (1.7, 1.8)$. The edge lengths of the bounding box in Fig. 4 along xyz axis are calculated as l_x, l_y and l_z, respectively and the scale factor s_x, s_y and s_z for shrinking M can be evaluated as Eq. (3.1):

$$s_x = \frac{l_x - D_{axial}}{l_x}, s_y = \frac{l_y - D_{axial}}{l_y}, s_z = \frac{l_z - D_{occlusion}}{l_z} \quad (3.1)$$

Intuitively, select the origin of local coordinate system as the scaling center. Use the symbol (V_{cx}, V_{cy}, V_{cz}) and (V'_x, V'_y, V'_z) represent the coordinate of the origin of the local coordinate system and that of the vertices of M', respectively, and (V'_x, V'_y, V'_z) is evaluated as Eq.(3.2) below:

$$(V'_x, V'_y, V'_z, 1) = (V_x, V_y, V_z, 1) \begin{bmatrix} s_x & 0 & 0 & 0 \\ 0 & s_y & 0 & 0 \\ 0 & 0 & s_z & 0 \\ (1-s_x)V_{cx} & (1-s_y)V_{cy} & (1-s_z)V_{cz} & 1 \end{bmatrix} \quad (3.2)$$

After the above treatment, smoothing step is further carried out to remove some features making it be smooth for putting on adhesive. In this paper, one simple smoothing scheme is adopted as Eq. (3.3):

$$P = \frac{1}{n}\sum_{i=0}^{n-1} Q_i(P) \quad (3.3)$$

Where $Q_i(P)$ are the 1-ring neighboring vertices of point P and n is the number of neighboring points. Fig. 5 shows the resultant abutment for a molar and an incisor using the above method.

4. Design of the crown

In the crown shape design, the shape of the initial abutment is preferred to change automatically with the modification of the crown shape. In this paper, we use direct manipulation of free-form deformation (DMFFD) method [3] to support the interactive design of the crown and guarantee the thickness requirement.

4.1. Direct manipulation of free-form deformation (DMFFD)

Before depicting the algorithm of direct manipulation of free-form deformation (DMFFD), we first introduce

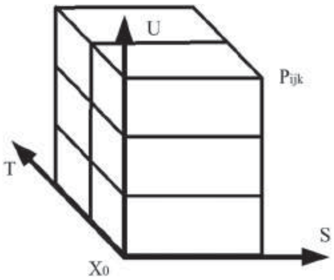

Figure 6. Establish the FFD's control lattice based on the local coordinate system.

free-form deformation (FFD) [16]. In the FFD algorithm, a control lattice shown in Fig. 6 is used to control the shape deformation.

The lattice includes one frame denoted as S,T and U and the origin is denoted as X_0, which is coincident with the origin O of the local frame in Fig. 3. For each model vertex V, a triple coordinate denoted by (s, t, u) in the frame is represented as below:

$$V = X_0 + sS + tT + uU \tag{4.1}$$

The coordinates s, t, u are evaluated as Eq. (4.2):

$$s = \frac{T \times U \bullet (V - X_0)}{T \times U \bullet S}, t = \frac{S \times U \bullet (V - X_0)}{S \times U \bullet T},$$
$$u = \frac{S \times T \bullet (V - X_0)}{S \times T \bullet U} \tag{4.2}$$

Where $0 < s < 1$, $0 < t < 1$, $0 < u < 1$, '$\bullet$' and '$\times$' stand by the vector dot product and cross product, respectively. The lattice control point P_{ijk} is calculated by Eq. (4.3) :

$$P_{ijk} = X_0 + \frac{i}{l}S + \frac{j}{m}T + \frac{k}{n}U \tag{4.3}$$

Where l, m and n are the numbers of the control lattice grids in the S, T and U direction, respectively. In Fig. 6, $l = 1, m = 2, n = 3$. The model vertices V (s, t, u) can be updated by the lattice control points using Eq. (4.4)

$$V = \sum_{i=0}^{l} \binom{l}{i} (1-s)^{l-i} s^i \left[\sum_{j=0}^{m} \binom{m}{j} (1-t)^{m-j} t^j \right.$$
$$\left. \left[\sum_{k=0}^{n} \binom{n}{k} (1-u)^{n-k} u^k P_{ijk} \right] \right] \tag{4.4}$$

It can be seen from the above formula, the modification of these control points in the lattice can change the shape of the model, but this scheme is not intuitive and one hopes to change the shape in an easier manner, in which one specific vertex of the model is selected and moved to the expected position. In order to meet this requirement, the DMFFD algorithm is proposed in [3] and its performance and advantage is well introduced by Menzal [10]. Noble [12] devised the NURBS basis function in place of the Bernstein basis such that DMFFD can be more flexible. Out of the easier interactive design consideration, Xu [19] proposed an extended DMFFD algorithm based on curves. In this paper, the method [3] is implemented and adopted to support the crown shape design. In the algorithm, some arbitrary vertices of the edited mesh model rather than control points in the lattice are selected and dragged to the expected locations and the other left vertices will be updated in the lease square sense.

The Eq. (4.4) can be rewritten in the matrix form, i.e., $V = BP$, where P stands for the matrix recording all control points, B represents the Bernstein basis matrix and the symbol ΔV is the modification of V. In DMFFD, the vertices of P rather than V are preferred to be modified, thus ΔV is regarded as known numbers and the movements amount of all the control points, i.e., ΔP are unknowns. The movement ΔP can be evaluated using well-known least square method as Eq.(4.5):

$$\Delta P = B^+ \Delta V \tag{4.5}$$

Where B^+ represents the pseudo-inverse matrix of B and P will be replaced by $P = P + \Delta P$. After updating P, all the model vertices will be re-calculated using the Eq. (4.4) with their corresponding (s, t, u) coordinate one by one. In our package, the above algorithm is used to design the shape of the crown by editing the initial standard tooth from the database.

4.2. Linkage free-form deformation algorithm (L-FFD)

For our specific application, linkage free form deformation (L-FFD) algorithm is proposed to guarantee the crown-abutment thickness requirement. In the proposed algorithm, the shape modification of the crown is proceeded using the above DMFFD algorithm and its deformation information together with the thickness constraint is considered when automatically deforming the corresponding abutment. The process flow of L-FFD algorithm is shown in Fig. 7.

In this paper, the initial abutment is first implanted together with the standard tooth in the position of the missing tooth; through our algorithm, one can modify the standard tooth freely without considering the shape modification of the initial abutment. The thickness at the specific vertex V of the tooth is regarded as the minimum distance from it to its corresponding abutment. As

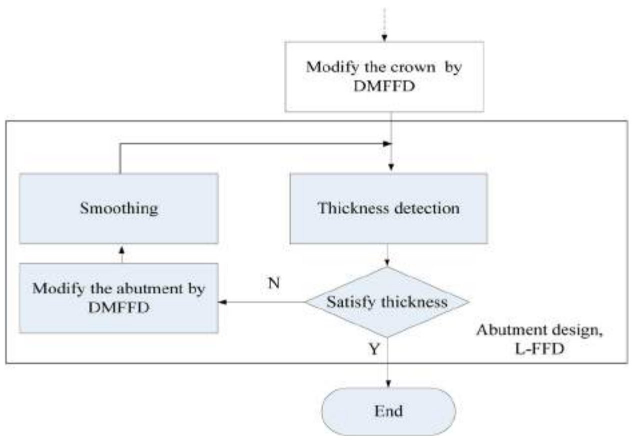

Figure 7. The flow of L-FFD.

the standard tooth and the abutment have been both pretreated as fine-mesh models and their triangle numbers are dense enough, the shortest Euclidean distance from V to the vertices of the abutment is taken as the thickness at V. During the design process of the crown, for efficiency and accuracy consideration, the lattice division number, i.e., l, m and n are empirically set as 10*10*10. Assume point Q on M is selected to be moved to change the shape of M. Its closest point on M' is marked as q. Assume Q is moved by $D(D_x, D_y, D_z)$. If the movement amount D is directly applied on point q, the anatomical morphology similarity of the crown and abutment will be not held, which is not conducive to the following porcelain process on the tooth or the thickness condition may be not satisfied. As M' is obtained by scaling M down with a certain ratio, M and M' are similar in the shape. Intuitively, the movement amount of q should be reduced with the same ratio scale. Thus, the movement amount of q is denoted by $d(d_x, d_y, d_z)$ and calculated by Eq.(4.6):

$$d_x = s_x \cdot D_x, d_y = s_y \cdot D_y, d_z = s_z \cdot D_z \tag{4.6}$$

The difference between D and d is denoted as $\Delta d(\Delta d_x, \Delta d_y, \Delta d_z)$ and $\Delta d = (D - d)$. The above treatment is a rough method and sometimes cannot guarantee the thickness requirement during the deformation. However, the thickness can be allowed to be varied within a range, i.e., 1.0 ~ 1.5 mm for the axial surface part and 1.5 ~ 2.0 mm for the occlusal surface part, so if the difference Δd is limited to be a range, the thickness condition can be met during the deformation. When generating the initial abutment, the intended value in the axial direction is D_{axial} and $2^*D_{occlusion}$ in the occlusal direction, so the limit movement in X and Y axes for Δd should be bounded by D_{axial}-1 and 1.5-D_{axial}. As Z axis denotes the occlusal direction, the limit value of Δd should be bounded by $2^*D_{occlusion}$-1.5 and 2-$2^*D_{occlusion}$. Once the component of Δd exceeds the above bounding range, the thickness requirement will not be met. If the modification of P moves beyond its limit, it means that the deformation of the tooth changes too much and doctors are suggested to choose other treatment options or generate the diagnosis dental model again. Fig. 8 shows three results with different treatment of Δd.

In Fig. 8 (b), $\Delta d = 0$ and the thickness requirements is not met and the anatomical similarity is not kept either. In Fig. 8 (c), the displacement amount of the abutment is proportional to that of the tooth, the result is acceptable when M is deformed slightly, but the thickness requirement is difficult to be satisfied for larger deformation of M. In Fig. 8 (d), limit displacement strategy works even for the large deformation of M as the thickness satisfies the requirement.

Lot of tests have been done using the above method, finding that in the case of large depression deformation on some tooth parts including deep grooves and ridges, there are still some probability chance of the thickness not meeting the requirement. For these special cases, some particular treatments should be done. Thus, one detection step will be added in L-FFD, once the thickness

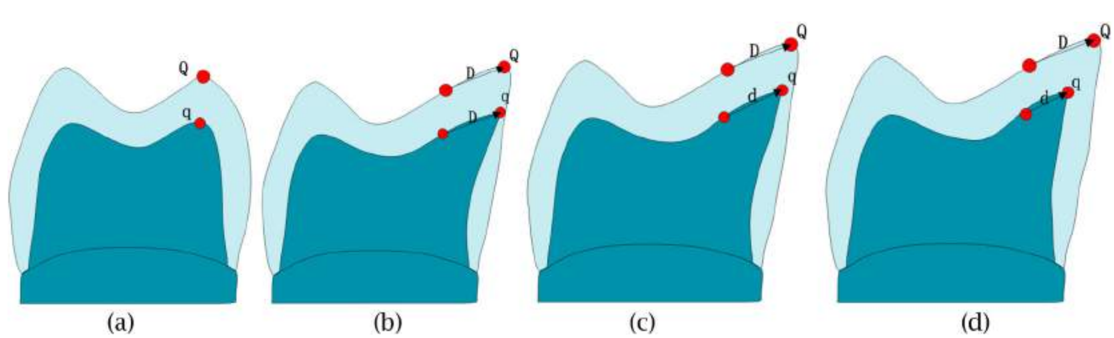

Figure 8. The limit displacement strategy for abutment in L-FFD, (a) Select control points Q on the crown and point q on the abutment for changing the shapes of the crown and abutment, respectively; (b) Q and q are applied with the same movement amount D; (c) q is applied with a scaled movement amount d; (d) the movement amount d is limited within a range.

requirement is not met, the local adjustment will be carried out: assume the abutment point ***r***'s thickness is not in the required range and the closest point on the crown is denoted as ***R***, and point ***r*** need to be moved along the direction (***r***-***R***) using DMFFD, and the movement amount is calculated as:

$$\Delta D = (|r - R| - D_{demand})^{*}1.5 \qquad (4.7)$$

Where D_{demand} is the preset thickness value. Here, DMFFD is adopted to complete the local adjustment. For the local adjustment, the grid numbers i.e., l, m and n is set to be 5*5*5 for efficiency consideration and the vertices number for processing will be significantly reduced than that of deforming the crown. After adjusting all unsatisfied points on the abutment, the surface of abutment may be not smooth, so the laplacian smoothing step will be performed. These three steps including thickness detection, modification by DMFFD and smoothing are alternately and iteratively done until the thickness requirement is met. In practice, after repeating 3 to 5 times, the ideal thickness can be achieved and the surface of abutment is smooth enough.

5. Implementation and examples

Currently, EXOCAD and 3 Shape are most widely used in practice, in which operators should take great care to watch out for the thickness requirement by repeatedly editing the shape of the abutment or the crown. In more details, after finishing the design of the crown, the abutment shape edit will be followed. Actually, the thickness check procedure is tedious and time consuming (see Fig. 9): one should first construct a series of cutting planes in the interested regions and obtain two 2D sectioning profiles curves for the inner crown surface and the outer abutment surface, respectively.

The distance between these two profile curves are approximated as the abutment-crown thickness in this region. Once the distance being out of the required interval, the shape of abutment or the crown will be locally adjusted. In EXOCAD and 3 shape, the local modification will result in a global deformation for the abutment or the crown, thus these local cutting plane sampling inspection scheme needs skilled experiences and usually takes much time. However, the proposed algorithm supports one to focus on the crown shape design only and the thickness requirement will be automatically satisfied, saving lots of time.

To verify the effectiveness and efficiency of the proposed algorithm, it has been implemented by C++ and complied in VS2010; two typical testing cases, i.e. one incisor and one molar, are run on the PC with i5-6500 processor and 8G DDR4 memory. Fig. 10 visually shows the thickness distribution after our method. Fig. 10 (a) & Fig. 10 (d) are the initial abutments together with their corresponding standard teeth and Fig. 10 (b) & Fig. 10 (e) are the results after modification of the tooth crowns. From Fig. 9, it is found that the shape of the abutment is updated automatically with the change of the corresponding crowns; From the thickness distribution map in Fig. 10 (c) and Fig. 10 (f), we can find that the thickness of the incisor's axial surface part is between 1.26 mm and 1.41 mm and for the occlusal surface part, the thickness is between 1.70 and 1.85 mm, both of which satisfy the thickness requirements, i.e., 1.0 mm ∼ 1.5 mm for axial

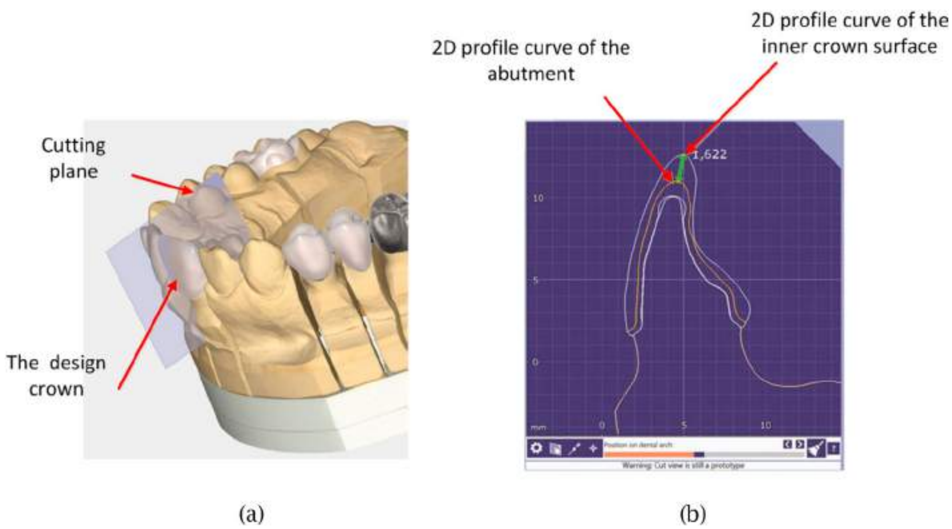

Figure 9. The thickness requirement check in EXOCAD system: a series of cutting planes are constructed in the areas of interest (Fig. 9(a)) and the distance of the 2D contours of the abutment and the inner crown surface (see Fig. 9(b)) is regarded as the thickness in this local region.

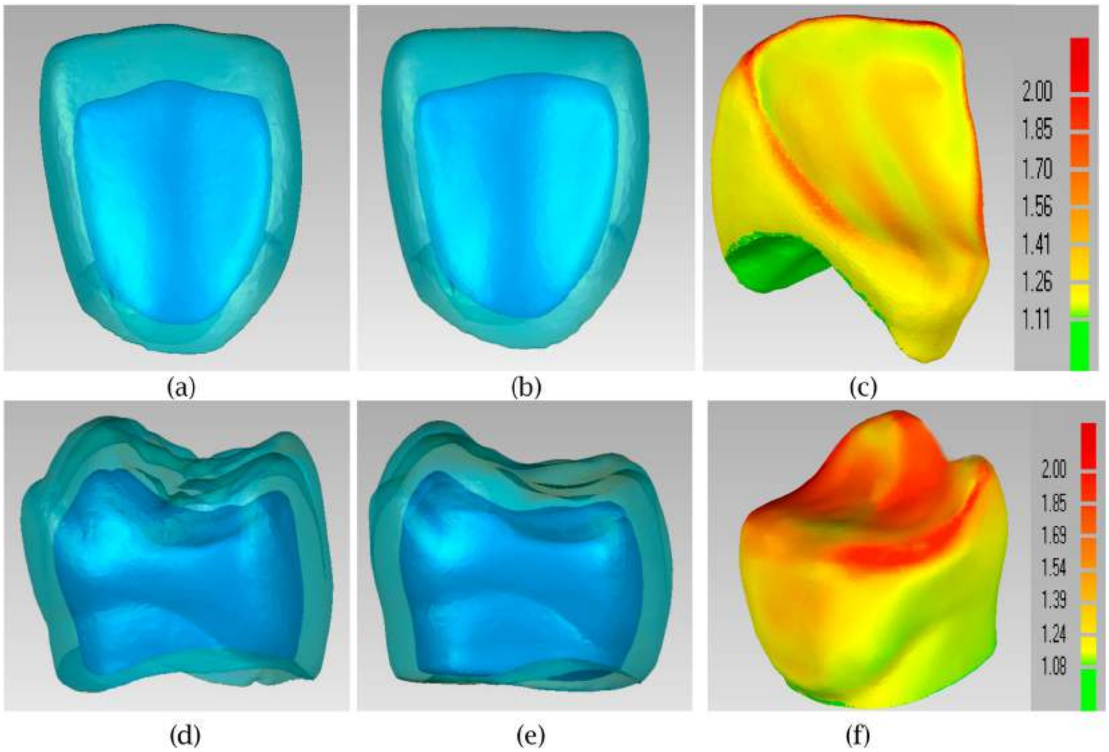

Figure 10. The thickness distribution after L-FFD:(a)&(d) the initial abutments and their corresponding standard tooth model; (b) &(e) the results after L-FFD are smooth enough; (c)&(f) the distance distribution map of (b)&(e) represents the thickness is within the required range.

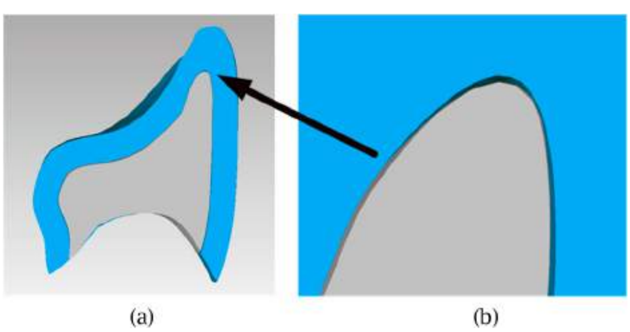

Figure 11. The generated inner crown surface by offsetting the corresponding abutment.

surface part and 1.50 mm ~ 2.0 mm for the occlusal surface part. For the molar, the thickness is also within the required range. Thus, the proposed algorithm can ensure both the smoothness for abutments and the abutment-crown thickness requirement is also met automatically.

After obtaining the final abutment shape, mesh surface-offsetting method is used to generate the inner crown surface by offsetting the corresponding abutment. More explicitly, for each vertex of the abutment, the vertex is moved outward along its normal direction by 0.05 mm and the generated space between the inner crown and the abutment will be used for adhesive, by which the crown and the abutment will be glued together. As the abutment for offsetting is smooth enough and offsetting amount is very small, the collision will never occur and the generated inner crown surface is always acceptable. Fig. 11 shows the generated inner crown surface by offsetting the abutment, between which 0.05 mm exists.

The proposed algorithm can get an instant response, which is important for the crown design. Tab. 1 gives the statistics of the running time.

From Tab.1, we can find that DMFFD algorithm can support an instant response, 78 ms for the incisor crown

Table 1. Running time for the L-FFD algorithm.

Figure	Vertex number/ triangle number	DMFFD for crown (ms)	DMFFD for abutment (ms)	Thickness detection (ms)	Smoothing (ms)	Number of iteration
Fig. 10 (a)	9084/18088	78	78	5	20	3
Fig. 10 (d)	12798/25843	98	98	5	21	5

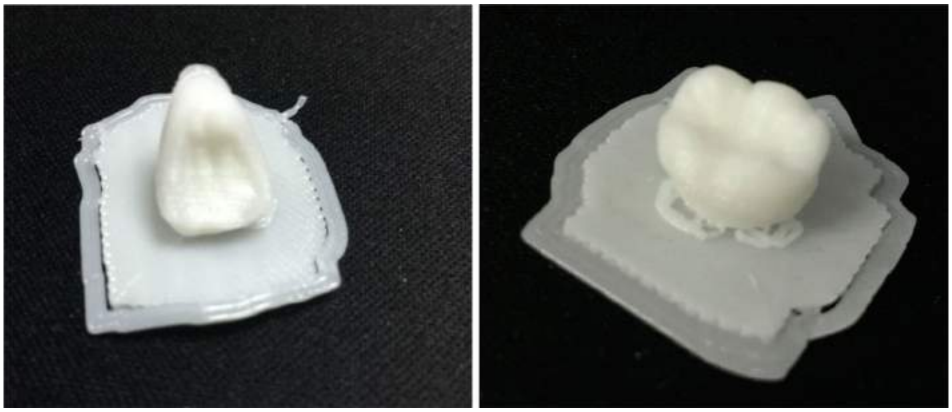

Figure 12. The 3D printing results of the incisor abutment and the first molar abutment designed by L-FFD.

design and 98 ms for the molar crown design, which is important for performing the crown design in an interactive manner. The abutment design is completed automatically, three steps, i.e., DMFFD, thickness detection and smoothing are alternately and repeatedly carried out. Each iteration takes 103 ms for the incisor abutment and 124 ms for the molar abutment. Three iterations and five iterations are needed for obtaining the results in Fig. 10(b) and Fig. 10 (e), respectively. Fig. 12 shows the 3D printing results of the incisor abutment and the first molar abutment designed by L-FFD.

6. Conclusions

In this paper, a novel algorithm is proposed to design the crown together with the abutment shapes simultaneously; the shape of abutment can be automatically changed with the modification of the corresponding tooth crown. The final deformed abutment is smooth and most importantly the thickness between the abutment and the tooth can satisfy the requirement, which is currently met by the sophisticated manual edit on the shape of the abutment and the tooth crown. Through this work, the tooth crown design efficiency can be sped up greatly as there is no need to consider the thickness constraints with great care. Our testing cases have shown that the proposed the algorithm is efficient and valid. Besides the application of tooth design, the proposed algorithm can be also used in other engineering applications in which the thickness is needed. In the future work, more efficient deformation method rather than DMFFD can be studied, as DMFFD algorithm need the lattice number not exceeding the preset number otherwise the algorithm performance will be impaired significantly.

Acknowledgements

This work is supported by the Natural Science Foundation of China (Grant No. 61662006), the Fundamental Research Projects of Shenzhen (Grant No. JCYJ20140417172620448) and the funding of Guangxi province 100 oversea talent plan.

ORCID

Xun Li http://orcid.org/0000-0003-1259-614X
Ming Chen http://orcid.org/0000-0003-1517-1753

References

[1] Blanz, V., Mehl, A., Vetter, T., Seidel, H.-P.: A statistical method for robust 3D surface reconstruction from sparse data, international Symposium on 3d Data Processing, Visualization and Transmission, 21, 2004, 293-300. https://doi.org/10.1109/TDPVT.2004.1335212
[2] Chao, Y.-L: Prosthodontics, Book, People's Medical Publishing House, Beijing, 2011.
[3] Hsu, W.-M., Hughes, J.-F., Henry, M.: Direct manipulation of free-form deformations, ACM Siggraph Computer Graphics, 26(2), 1994, 177–184. https://doi.org/10.1145/133994.134036
[4] Jiang, X.-T., Dai, N., Cheng, X.-S., Wang, J., Peng, Q.-J.: Robust Tooth Surface Reconstruction by Iterative Deformation, Computers in Biology and Medicine, 1(68), 2016, 90–100. http://doi.org/10.1016/j.compbiomed.2015.11.001
[5] Kollmuss, M., Kist, S., Goeke, J., Hichel, R., Huth, K.: Comparison of chairside and laboratory CAD/CAM to conventional produced all-ceramic crowns regarding morphology, occlusion, and aesthetics, Clinical Oral Investigations, 20(4), 2016, 791–797. https://doi.org/10.1007/s00784-015-1554-9
[6] Lipman, Y., Sorkine, O., Levin, D., Cohen, D.: Linear rotation-invariant coordinates for meshes, ACM Transactions on Graphics, 24(3), 2005, 479–487. https://doi.org/10.1145/1186822.1073217
[7] Larsson, C., Madhoun, S., Wennerberq, A., Steyern, P.: Fracture strength of yttria-stabilized tetragonal zirconia polycrystals crowns with different design: an in vitro study, Clinical Oral Implants Research, 23(23), 2012, 820–826. https://doi.org/10.1111/j.1600-0501.2011.02224.x
[8] Marchack, B.-C., Vidjak, F.-M., Futatsuki, V.: A simplified technique to fabricate a custom milled abutment, Journal

of Prosthetic Dentistry, 98(5), 2007, 416–417. http://doi.org/10.1016/S0022-3913(07)60127-9
[9] Mehl, A., Blanz, V., Hichel, R.: Biogeneric tooth: a new mathematical representation for tooth morphology in lower first molars, European journal of oral sciences, 113(4), 2005, 333–340. https://doi.org/10.1111/j.1600-0722.2005.00224.x
[10] Menzel, S., Olhofer, M., Sendgoff, B.: Direct Manipulation of Free Form Deformation in Evolutionary Design Optimisation, Parallel Problem Solving from Nature - PPSN IX, 4193, 2006, 352–361. https://doi.org/10.1007/11844297_36
[11] Miyazaki, T., Hotta, Y., Kunii, J., Kuriyama, S., Tamaki, Y.: A review of dental CAD/CAM: current status and future perspectives from 20 years of experience, Dental materials journal, 28(1), 2009, 44–56. http://doi.org/10.4012/dmj.28.44
[12] Noble, R.-A., Clapworthy, G.-J., Direct Manipulation of Surfaces using NURBS-Based Free-Form Deformations, IEEE international conference on information visualization, IEEE, London, 1999, 238-243. https://doi.org/10.1109/IV.1999.781565
[13] Steinbrecher, T., GertH, M.: Dental inlay and onlay construction by iterative laplacian surface editing, Symposium on Geometry Processing, 2008, 1441-1447. http://doi.org/10.1111/j.1467-8659.2008.01284.x
[14] Sorkine, O., Cohen, D., Lipman, Y., Alexa, M.: Laplacian surface editing, Euro graphics/ACM SIGGRAPH symposium on Geometry processing, 2004, 175-185. https://doi.org/10.1145/1057432.1057456
[15] Song, Y.L.: Research on the key Technologies in Computer-Aided Dental Design, Ph.D., Thesis, Tianjin University, Tianjin, 2006.
[16] Sederberg, T.W., Parry, S.R.: Free-form deformation of solid geometric models. In ACM SIGGRAPH computer graphics. 1986, 151-160. https://doi.org/10.1145/15922.15903
[17] Zhang, C.D., Dai, N., Liao, W.H.W.: Partially missing dental occlusion surface adaptive reconstruction algorithm. Chinese Journal of Biomedical Engineering, 31(2), 2012, 203-210. https://doi.org/10.3969/j.issn.0258-8021.2012.02.007
[18] Zheng, S.x., Li, J., Sun, Q.F.: A novel 3D morphing approach for tooth occlusal surface reconstruction. Computer-Aided Design, 43(3), 2011, 293-302. http://doi.org/10.1016/j.cad.2010.11.003
[19] Xu, G., Hui, K.-C., Ge, W.-B., Wang, G.-Z.: Direct manipulation of free-form deformation using curve-pairs, Computer-Aided Design, 45(3), 2013, 605–614. https://doi.org/10.1016/j.cad.2012.09.004